Real-Time Electrochemical PCR with a DNA Intercalating Redox Probe

ARTICLE *in* ANALYTICAL CHEMISTRY · MARCH 2011

Impact Factor: 5.64 · DOI: 10.1021/ac1033374 · Source: PubMed

5 AUTHORS, INCLUDING:

Thibaut Deféver
Independent Researcher
5 PUBLICATIONS **64** CITATIONS
SEE PROFILE

David Evrard
Paul Sabatier University - Toulouse III
26 PUBLICATIONS **350** CITATIONS
SEE PROFILE

Damien Marchal
Paris Diderot University
36 PUBLICATIONS **458** CITATIONS
SEE PROFILE

Benoît Limoges
Paris Diderot University
118 PUBLICATIONS **2,326** CITATIONS
SEE PROFILE

analytical chemistry

ARTICLE

pubs.acs.org/ac

Real-Time Electrochemical PCR with a DNA Intercalating Redox Probe

Thibaut Defever, Michel Druet, David Evrard, Damien Marchal,* and Benoit Limoges*

Laboratoire d'Electrochimie Moléculaire, UMR CNRS 7591, Université Paris Diderot, 15, rue Jean-Antoine de Baïf, 75205 Paris Cedex 13, France

Supporting Information

ABSTRACT: The proof-of-principle of a nonoptical real-time PCR method based on the electrochemical monitoring of a DNA intercalating redox probe that becomes considerably less easily electrochemically detectable once intercalated to the amplified double-stranded DNA is demonstrated. This has been made possible thanks to the finding of a redox intercalator that (i) strongly and specifically binds to the amplified double-stranded DNA, (ii) does not significantly inhibit PCR, (iii) is chemically stable under PCR cycling, and (iv) is sensitively detected by square wave voltammetry during PCR cycling. Among the different DNA intercalating redox probes that we have investigated, namely, methylene blue, Os[(bpy)$_2$phen]$^{2+}$, Os[(bpy)$_2$DPPZ]$^{2+}$, Os[(4,4′-dimethyl-bpy)$_2$DPPZ]$^{2+}$ and Os[(4,4′-diamino-bpy)$_2$DPPZ]$^{2+}$ (with bpy = 2,2′-bipyridine, phen = phenanthroline, and DPPZ = dipyrido[3,2-a:2′,3′-c]phenazine), the one and only compound with which it has been possible to demonstrate the proof-of-concept is the Os[(bpy)$_2$DPPZ]$^{2+}$. In terms of analytical performances, the methodology described here compares well with optical-based real-time PCRs, offering finally the same advantages than the popular and routinely used SYBR Green-based real-time fluorescent PCR, but with the additional incomes of being potentially much cheaper and easier to integrate in a hand-held miniaturized device.

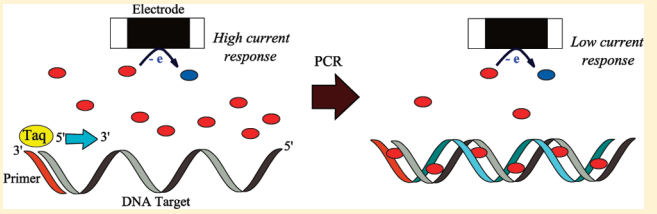

Since its invention in the early 90s,[1] real-time PCR has become an indispensable tool in many fields of molecular diagnostics, including determination of viral or bacterial loads in clinical samples, identification and titers of germs in food, diagnosis of tumors, gene expression analysis, or forensic analyses.[2] The key to its success is that the amplification of a target DNA sequence is quantified as it accumulates in the reaction solution, thereby avoiding time-consuming post-PCR analysis. Moreover, this closed-tube analysis can be used to detect a DNA sequence with enhanced accuracy and speed, and it can provide a quantitative result without risk of cross-contaminations by amplified-PCR products.

To date, all of the commercialized real-time PCR instruments are based on the optical detection of a fluorescent reporter molecule that produces an increase (or occasionally a decrease) of fluorescence as the reaction proceeds.[2] These fluorescent reporter molecules include dyes that bind to double-stranded DNA (e.g., SYBR Green)[3] or sequence-specific fluorescent oligonucleotide probes[4] that fluoresce upon specific hybridization with the amplified DNA product. The resulting kinetic plot of fluorescence versus cycle number thus provides a way to monitor the PCR reaction in its early exponential phase, and it offers a route to identify and quantitatively determine a DNA target over more than 6 orders of magnitude of concentration ranges.[2]

Regardless of their great success for analyzing nucleic acids, real-time PCR instruments currently on the market are based on complex and delicate optical components that leads to rather bulky, fragile, and costly instruments, thereby restricting their use to clinical and research laboratories. With the aim to develop a real-time PCR technology for point-of-care DNA analysis in a hand-held instrument, an interesting prospect is to replace optical-based detection schemes with more robust, less expensive and easier to miniaturize nonoptical sensing methods. Among the few attempts aimed at achieving this goal,[5,6] electrochemical detection methods appear the most promising because they require minimal instrumentation, low electrical power supply and they can be easily integrated with microelectronics in a miniaturized chip-based format.[6]

Hsing and coll were the first to demonstrate the possibility to monitor electrochemically DNA amplification during PCR.[6e] Their detection strategy was based on the coupling of a solid-phase PCR amplification with the electrochemical detection of a surface-incorporated redox-labeled base. However, the inconvenient with this approach are the poor amplification efficiency of the on-electrode PCR that leads to a linear rather than an exponential growth of signal, the need to immobilize the primer on the electrode surface, which is rather laborious and time-consuming, and the memory effects or instability of the primer-modified electrodes that restrict their use to a scarce number of measurements during a PCR experiment. In view of these limitations, a better strategy would be to develop an electrochemical

Received: December 24, 2010
Accepted: January 9, 2011
Published: January 31, 2011

Scheme 1. (Left) Scheme's Principle of the Real-Time Electrochemical Monitoring of DNA Amplification during PCR Using a ds-DNA Intercalating Redox Probe (Red Dots) and (Right) DNA Intercalating Redox Probes That Have Been Investigated in This Work

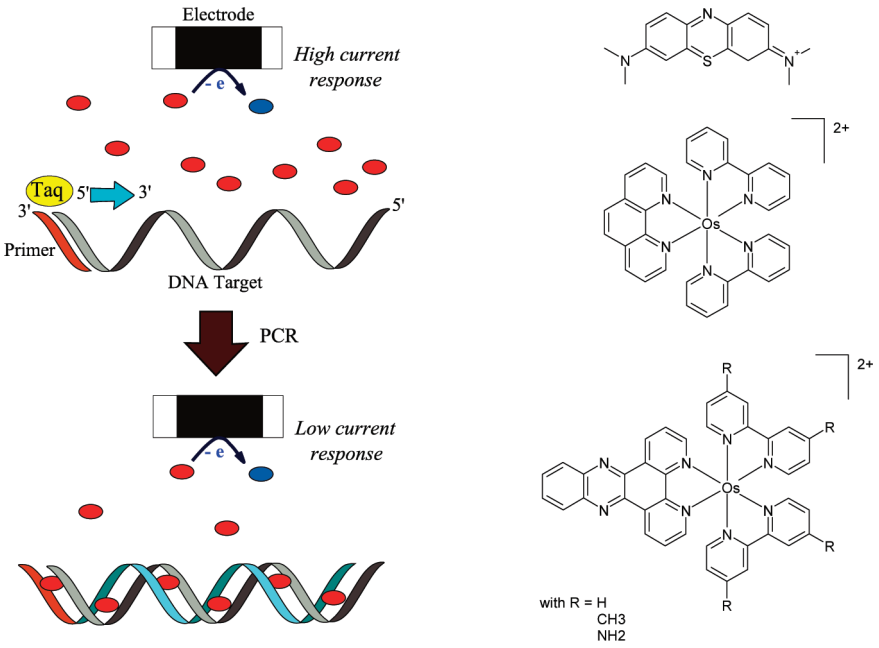

detection scheme that indirectly probes DNA polymerization in homogeneous solution instead of on the surface of an electrode. This is what we have recently proposed with the electrochemical detection of the exponential consumption of free electroactive deoxynucleoside triphosphates during a PCR reaction.[7] Using this method, it was possible to monitor DNA amplification at each PCR cycle in a multiplexed array of small closed-electrochemical cells (<50 μL of PCR mix per cell), and thus plot a complete kinetic PCR curve. However, in comparison with commercialized real-time fluorescent PCR, the electrochemical strategy was shown to suffer from a somewhat lack of sensitivity as well as specificity.[8] To overcome these limitations, we propose here an alternative strategy based on the use of a DNA intercalating redox probe (Scheme 1), which upon binding to the amplified double-stranded DNA (ds-DNA) becomes less electrochemically detectable (i.e., less accessible to an electron exchange with the electrode due to steric and/or diffusional constraints) compared with its free counterpart.[9] The principle is analogous to that of ds-DNA intercalating fluorescent dyes, except that the signal of the redox intercalator is exponentially decreased as the amount of amplified DNA template is raised with the number of PCR cycles.

EXPERIMENTAL SECTION

Reagents. The osmium complexes were synthesized according to published procedures.[10] The quantified biological extract of hCMV DNA template (2×10^5 copies/μL) was obtained from a MRC5 cell line extract infected by AD169 CMV stain. The hCMV DNA extraction was realized with QIAamp DNA Blood Mini kit (Qiagen). The concentrated amplicon of 283-bp hCMV DNA (2.6×10^{10} copies/μL) was obtained from standard PCR amplification of the biological extract. The copy number of hCMV target sequences contained in the concentrated amplicon was calibrated by gel electrophoresis. PCR products were electrophoresed on a 2% agarose gel and were visualized by ethidium bromide staining.

Electrochemical Cell Holder. The sample holder shown in Supporting Information (Figure S1) has been designed around a disposable array of eight independent electrochemical cells. The eight self-contained electrochemical cells were assembled from a eight-strip of polypropylene domed caps (ABgene) sealed over an array of 8 × 3 band-electrodes (a carbon working electrode, a carbon counter electrode and a Ag/AgCl reference electrode) screen-printed on a flexible planar polyethylene terephthalate sheet. For a tight seal of the strip caps over the planar polyester substrate, the eight electrochemical cells were sandwiched between an aluminum plate holder and a plastic plate holder clamped with six screws. Such an assembly allows definition of each cell a working electrode area of 0.02 cm^2, the latter being delimited by the inside diameter of the polyethylene cap apertures, and a working cell volume of 75 μL, allowing us to perform PCR with a reaction volume of 25−50 μL. The backside of the aluminum plate holder was mounted inside the chamber of a thermocycler (Swift Maxi thermal cycler from Esco). Once turned upside down and mounted flat on the planar metal heating block of the thermocycler, the eight electrochemical cells can be simultaneously scanned by square-wave voltammetry (SWV) at a defined time during each PCR cycle. Because of a significant thermal inertia brought by the plate holders, a maximal heating and cooling rate of ±1 °C/s was achieved.

Real-Time PCR Conditions for the hCMV DNA. Specific primers, provided by Argene (proprietary sequences), were used to amplify a 283-bp hCMV DNA fragment targeting UL83 gene coding for phosphoprotein pp65.[11]

The real-time electrochemical PCR of hCMV DNA were performed in (50 μL) Qiagen buffer (1×) containing 0.5 μM Os(bpy)2DPPZ^{2+}, 0.2 mM of each dNTP, 0.25 μM of each forward and reverse primers, 5 units of HotStartTaq polymerase (Qiagen), and 2.5 μL of serial dilution of the calibrated 283-bp

dx.doi.org/10.1021/ac1033374 |Anal. Chem. 2011, 83, 1815–1821

hCMV DNA amplicon (2.6×10^{10} copies/μL) or 5 or 0.5 μL of the quantified biological extract of hCMV DNA (2×10^5 copies/μL). The PCR was performed according to the following thermal cycling: preheating period of 15 min at 95 °C, followed by a maximum of 45 cycles of 95 °C for 60 s, 58 °C for 120 s, and 72 °C for 120 s. The square wave voltammograms were recorded at 72 °C during the extension step of each PCR cycle.

The conventional fluorescent-based method (TaqMan-based real-time PCR) was performed on a Rotor-Gene (Corbett Life Science). The PCR reaction was performed in 25 μL containing Qiagen buffer 1×, 0.2 mM of each dNTP, 0.5 μM of specific primers, 0.1 μM of specific probe (primers and probe provided by Argene), 1.875 units/PCR of HotStartTaq polymerase (Qiagen), and 10 μL of standard diluted solutions of the quantified biological extract of hCMV DNA template (final quantity ranging from 10 to 10^5 copies per assay). The PCR was performed at 95 °C for 15 min, followed by 45 cycles at 95 °C for 10 s and 60 °C for 40 s. The acquired fluorescence was measured during the step at 60 °C.

With the aim to compare the calibration plots obtained with both the TaqMan- and electrochemical-based real-time PCR, the cycle threshold values, C_t have been systematically determined using a signal/noise ratio of 3.

Electrochemical Measurements. Cyclic voltammetry was carried out with a PST20 Autolab potentiostat (Eco-Chemie) interfaced to a PC computer. For the square wave voltammetry, a homemade 8-channel multiplexed potentiostat synchronized to the thermal cycles of the PCR has been used. With such equipment it was possible to scan by SWV the 8 electrochemical cells quasi-simultaneously at the end of each elongation step of PCR cycle. The SWV technique was chosen for its higher sensitivity and also its relatively faster signal acquisition compared with other electrochemical methods. The square wave parameters were as follow: square-wave frequency of f = 300 Hz, pulse amplitude of ΔE_p = 25 mV, and potential step increment of E_{SW} =1 mV. Under these parameter conditions, it takes less than 5 s to scan the overall 8-cells of the array by SWV using our homemade multiplexed potentiostat.

The screen-printed electrodes were prepared from a semi-automatic screen-printer (Presco, USA), using carbon (PF 407A) and silver (418SS) carbon inks (Acheson Colloid).

Normalization of kinetic PCR plot was achieved by first correcting the small current drift occurring in the absence of specific signal decrease by, for example, subtracting a least-squares fitted line across the first cycles, and then by offsetting the data sets to align the value of these corrected cycles.

RESULTS AND DISCUSSION

For a successful demonstration of the method, the intercalating redox probe has to satisfy the following specifications: (i) to have a strong and preferential binding for the amplified ds-DNA, (ii) to be sensitively detected by a suitable electrochemical method within a few seconds, (iii) to be chemically stable during the overall thermal PCR cycles, and (iv) not inhibit PCR. We have thus investigated several DNA intercalating redox probes. The first ones were osmium bipyridine-based complexes bearing one dipyridophenazine ligand, that is, $Os(bpy)_2DPPZ^{2+}$, $Os(4,4'\text{-dimethyl-bpy})_2DPPZ^{2+}$, and $Os(4,4'\text{-diamino-bpy})_2DPPZ^{2+}$ (with bpy =2,2′-bipyridine, and DPPZ = dipyrido[3,2-a:2′,3′-c]phenazine). These complexes have been described as to selectively and strongly intercalate into duplex DNA (binding constant, K_b > 10^6 M^{-1}) thanks to their planar DPPZ ligand that can stack between the base pairs of DNA helix.[12,13] Moreover, they can reversibly exchange one-electron at a handy standard potential (E^0 ranging from 0.1 to 0.8 V vs SCE) and they are recognized as being highly chemically stable. We have also chosen to examine two other redox molecules with lower DNA binding affinities, the methylene blue (MB) and the $Os(bpy)_2phen^{2+}$ (with phen = phenanthroline). The MB compound was also selected because it was recently proposed as a DNA binding redox probe for an electrochemical-based PCR detection scheme whose concept is similar to the one proposed here, except that the current response during PCR amplification was monitored in a continuous flow-through microfluidic PCR device equipped with discrete electrochemical cells along a serpentine microchannel.[14] However, as will be shown in our nonflow real-time electrochemical PCR and contrary to what was previously stated, the principle of the method does not work with MB for the reason of its too poor ds-DNA binding affinity, a result that was corroborated by the experiments with the $Os(bpy)_2phen^{2+}$ which has similar low DNA binding properties.

To demonstrate the feasibility of the approach, a disposable array of eight miniaturized self-contained electrochemical cells implemented in a standard programmable thermal cycler was used. The system is similar to the one previously used by us (see Figure S1 in the Supporting Information),[7] except that here the eight multiplexed electrochemical cells were scanned by square-wave voltammetry (SWV) at a defined time during each PCR cycle.

The selected redox probes were first tested for their ability to inhibit (or not) PCR at micromolar concentrations (i.e., within the 0.2−20 μM range). Inhibition effects were evaluated by gel electrophoresis of the end-PCR product generated in standard microtubes from the PCR amplification of a 283-bp DNA sequence of human cytomegalovirus (hCMV) (see Figures S3−S6 in the Supporting Information). In contrast to MB and $Os(bpy)_2phen^{2+}$ which did not show any significant inhibition within the concentration range tested, the $Os(4,4'\text{-diamino-bpy})_2DPPZ^{2+}$ and $Os(4,4'\text{-dimethyl-bpy})_2DPPZ^{2+}$ were observed to fully inhibit PCR even at the lowest concentration of 0.2 μM, whereas for the $Os(bpy)_2DPPZ^{2+}$ the inhibition was only obvious at concentrations higher than 5 μM. The systematic PCR inhibition by redox probes bearing a DPPZ ligand is an indication of their strong intercalation to ds-DNA, which therefore could hinder to some extent the copying of DNA by polymerase. Inhibition of PCR by the probe added to the PCR mix is a well-identified problem for real-time fluorescent PCRs based on intercalating dyes.[15] For example, SYBR Green inhibits PCR (in a concentration-dependent manner) at concentrations greater than a few micromolars.[15a] Therefore, the best way to reduce as much as possible PCR inhibition consists of diluting the concentration of the intercalator, but not too much to have a detectable signal with reasonable amplitude. In our case, micromolar concentration ranges of redox probe can be easily detected by SWV with a relatively good signal/noise ratio (detection limit ~5 nM), but for the reason that at these levels of concentration the $Os(4,4'\text{-diamino-bpy})_2DPPZ^{2+}$ and $Os(4,4'\text{- dimethyl-bpy})_2DPPZ^{2+}$ fully inhibit PCR, these two latter probes were then discarded for the further experiments.

Another important prerequisite of the method is to have stable and reproducible electrochemical responses under thermal PCR cycling conditions. The SWV responses of $Os(bpy)_2phen^{2+}$, $Os(bpy)_2DPPZ^{2+}$, and MB were, therefore, investigated at

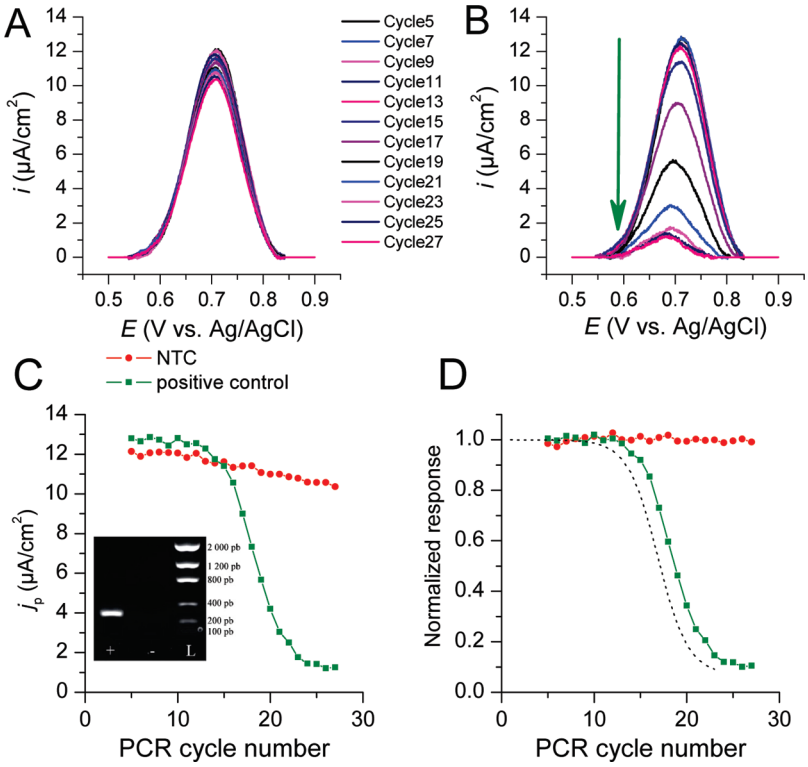

Figure 1. (A, B) Series of SWV curves (f = 300 Hz, ΔE_p = 25 mV, and E_{SW} = 1 mV) recorded during the PCR amplification of (A) a negative (no template) and (B) positive control (10^8 copies) of hCMV DNA template. The experiments were performed in 50 μL PCR mix containing 0.5 μM $Os[(bpy)_2DPPZ]^{2+}$. The thermal cycling parameters were 15 min at 95 °C followed by 28 thermal PCR cycles of 60 s at 95 °C, 120 s at 58 °C and 120 s at 72 °C. The SWV curves were acquired at the end of every 72 °C heating phase (for clarity, only few SWV scans were overlaid). (C) Plot of the SWV peak current density j_p as a function of cycle number. (D) Same as in C but after baseline correction and normalization. Inset: gel electrophoresis image of the end-PCR product of (+) positive control and (−) NTC. L: DNA ladder. Black dotted line: theoretical curve using $K_b = 10^5$, s = 3, C_I = 0.5 μM, ε = 1.85, and $N_c = 10^8$ copies.

micromolar concentrations under conditions that mimic thermal PCR cycling. A stable SWV peak current density (j_p) as a function of the cycle number was obtained for both the $Os(bpy)_2phen^{2+}$ and $Os(bpy)_2DPPZ^{2+}$, whereas a steady decrease was observed for MB (Figures S7−S8 in the Supporting Information). This latter result suggests some chemical degradation of MB during thermal cycling.

The three redox probes $Os(bpy)_2phen^{2+}$, $Os(bpy)_2DPPZ^{2+}$, and MB were next evaluated for their ability to give, at a defined number of PCR cycles, an exponential SWV peak current decrease during PCR amplification of a positive control of hCMV DNA (we used a 283-bp amplicon as template) and no decrease for a negative template control sample (NTC). The electrochemical kinetic PCR curves (i.e., SWV peak current densities j_p as a function of PCR cycle number) are reported in Figure 1 and in Supporting Information (Figures S9 and S10). Despite the presence of an intense 283-bp DNA band on the post-PCR gel images that signify successful PCR amplifications of positive controls, we were unable to obtain a significant difference between the positive and negative kinetic PCR plots, for both MB and $Os(bpy)_2phen^{2+}$. These results were in stark contrast to those obtained with the $Os(bpy)_2DPPZ^{2+}$ compound for which, at a defined number of PCR cycles, the occurrence of a clear and well-defined exponential decay of j_p was observed for the positive control, whereas there was no change for the NTC. The difference was even clearer after the kinetic PCR plots were baseline corrected and normalized (Figure 1D). The absence of signal decrease with both the MB and $Os(bpy)_2phen^{2+}$ probes can be explained by their too low DNA-binding affinity compared with that of $Os(bpy)_2DPPZ^{2+}$. The binding affinity of MB to different genomic DNAs has been determined by several groups using spectrophotometric titrations, and Kb values ranging from 10^4 to 10^5 M^{-1} at 20−25 °C were obtained, depending on the ionic strength of the solution and the DNA base composition.[16] The affinity binding of $Os(bpy)_2phen^{2+}$ was not available in literature, but it is expected to be not very different to that of $Ru(bpy)_2phen^{2+}$, for which a K_b value of 8×10^3 M^{-1} at 25 °C (10 mM phosphate buffer) has been reported.[17] These moderates DNA-binding affinities are significantly lower than those of intercalating dyes used for real-time fluorescent PCR[18], and they are probably lowered at the temperature measurement, that is, 72 °C.[19] Concerning the $Os(bpy)_2DPPZ^{2+}$, we have determined its ds-DNA-binding constant in a PCR buffer at room temperature and a value of $K_b = 5 \times 10^6$ M^{-1} was found (see Supporting Information). This value is in good agreement with that previously determined for calf thymus DNA ($K_b = 4 \times 10^6$ M^{-1}),[20] but also 2 orders of magnitude higher than MB. Given these considerations, a simple calculation based on a classical law of action mass including a predetermined number of noncooperative binding sites per unit of ds-DNA can provide a rough estimation of the relative concentrations of free and DNA-bound complex in the bulk PCR solution (see eq S2 in Supporting Information) and therefore a possibility to evaluate the percentage of signal decrease. If we assume that the concentration of DNA product (in nucleotide phosphate) at the end of PCR is on average of several tens of

dx.doi.org/10.1021/ac1033374 |*Anal. Chem.* 2011, 83, 1815–1821

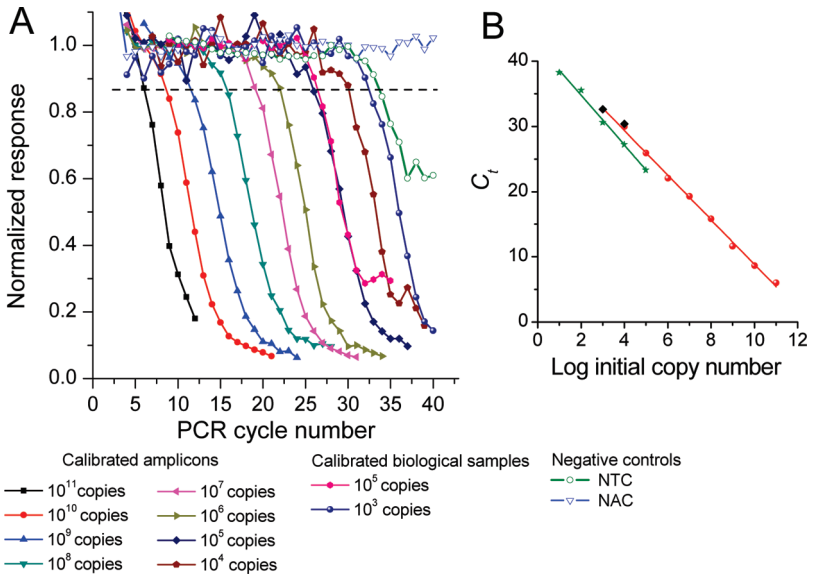

Figure 2. (A) Real-time electrochemical-based PCR curves for a 10-fold dilution series of 283-bp hCMV target DNA (the number of initial target copies are mentioned on the figure). The horizontal dashed line indicates the threshold level used to establish the C_t values. (B) Standard calibration plots of C_t vs the logarithmic input of hCMV copies for (red ●, black ♦) electrochemical-based real-time PCR and (green ★) conventional fluorescence-based real-time PCR (using TaqMan probes in a Rotor-Gene instrument). The data were obtained from serial dilutions of (green ★, black ♦) a quantified biological extract of hCMV DNA template (2×10^5 copies/μL) or (red ●) a calibrated mother solution of 283-bp hCMV DNA amplicon (2.6×10^{10} copies/μL).

micromolars under optimal conditions, and that the starting concentration of intercalator is fixed at 1 μM, the calculation gives less than few percents decrease in free intercalator concentration when using $K_b = 5 \times 10^3$ M^{-1} (a value that might correspond to that of MB at 72 °C in a PCR buffer), and more than 80% decrease with a K_b value 100-fold higher. To definitely confirm that the K_b value of $Os(bpy)_2DPPZ^{2+}$ is at the origin of the almost complete extinction of the electrochemical response observed in Figure 1, we have calculated the theoretical kinetic PCR plot by assuming that, at 72 °C, K_b should be ~50-fold lower than at room temperature, that is, $\sim 10^5$ M^{-1}.[19] For such purpose, we have combined the law of action mass to the basic equation of PCR kinetics (see eq S4 in Supporting Information).[21] The resulting theoretical curve reported in Figure 1D finally predicts quite well the amplitude of signal decrease as well as to some degree the start of signal decrease.

The next objective was to evaluate the analytical performances of the method and its ability's to quantify naturally occurring sequences of hCMV DNA from biological samples, and then to compare with conventional fluorescent methods. A series of kinetic PCR curves were thus generated from 10-fold serial dilutions of a calibrated solution of 283-bp hCMV DNA amplicon or a quantified biological extract of hCMV DNA template (Figure 2). As expected, we observed that the target number added to each reaction correlated to the cycle number where signal decrease crossed a fixed threshold value (C_t). A plot of C_t vs $\log_{10}$ initial copies of hCMV DNA (Figure 2B) gives a representative linear standard curve (over 8-$\log_{10}$ range) with an amplification efficiency of $\varepsilon = 1.95$ (which is close to the theoretical value of 2). In contrast to the very stable response of the no amplification control (NAC, i.e. control where one of the primers was omitted), a response decrease beyond the 33rd PCR cycle was obtained for the NTC, suggesting the occurrence of nonspecific amplification of primer-dimers. In view of this nonspecific response, a detection limit of $\sim 10^3$ copies of initial target can be estimated. A comparison to the standard curve obtained with a conventional TaqMan-based real-time PCR shows that the sensitivity of the electrochemical method is, within a factor 2, comparable to that of fluorescence (Figure 2B). The detection limit was however better with the TaqMan real-time PCR for the reason that the latter is not affected by the generation of primer-dimers. Nevertheless, by analogy with PCR based on intercalating fluorescent dyes,[22] it is reasonable to believe that a lower detection limit can be achieved by PCR optimization and the design of a device with a lower thermal inertia. In order to test the reproducibility, a series of real-time electrochemical PCR experiments ($n = 15$) has been done, starting from a same amount of DNA target (10^7 initial copies), and an average threshold value of 19.2 cycles with a relative standard deviation of ±0.6 cycles was obtained, corresponding thus to a relative standard error of 3%.

An interesting aspect of real-time PCRs that use intercalating dyes is the possibility to differentiate at the end of PCR full length amplicons from shorter products (such as primer-dimers) by a DNA melting curve analysis.[3b] It was thus tempting to test this possibility with our electrochemical approach. For such purpose, a SWV scan was recorded once every 0.5 °C during a linear ramp of temperature (0.5 °C/min) that was immediately started after achieving the PCR. As expected, the resulting SWV peak current response (i_p) of the positive control as a function of temperature (Figure 3) starts from a value close to zero and rises suddenly when the temperature has reach the melting temperature of the ds-DNA product loaded with its intercalator (~89 °C). This is in agreement with the release of the intercalated redox probe from ds-DNA during DNA dissociation, which consequently becomes more easily detectable. The melting curve obtained with the NTC also shows a significant increase of the current, but at a much lower temperature (~78 °C), a behavior that was attributed to the dissociation of nonspecifically amplified primer-dimers. The positive first derivative plot finally provides characteristic peaks localized at well-defined temperature, making it thus easier to discriminate target amplicons from other nonspecifically amplified DNA products.

dx.doi.org/10.1021/ac1033374 |*Anal. Chem.* 2011, 83, 1815–1821

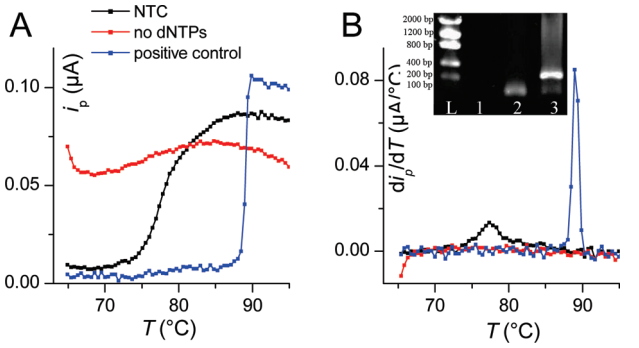

Figure 3. (A) Electrochemical post-PCR melt curves representing the SWV peak current, i_p, as a function of temperature, T, for one positive sample (10^7 copies), and two negative controls (i.e., a first one without template and a second one without dNTPs). (B) Positive first-derivative analyses (di_p/dT) of the melt curves shown in (A). Inset: Gel electrophoresis image of the post-PCR solution of (1) NAT, (2) NTC, and (3) the positive control. L: DNA ladder.

CONCLUSION

In conclusion, the proof-of-principle of a nonoptical real-time PCR method based on the electrochemical monitoring of a redox intercalating probe has been demonstrated. This has been made possible thanks to the finding of a stable redox probe that is able to bind strongly to ds-DNA without considerably inhibiting PCR. The methodology described here compares well with optical-based real-time PCRs, offering finally the same advantages than the popular and routinely used SYBR Green-based real-time fluorescent PCR, but with the additional incomes of being potentially much cheaper and easier to integrate in a hand-held miniaturized systems, such as in a microchip platform[6e] or in a microfluidic device.[6a] Work is in progress aimed at achieving this goal.

ASSOCIATED CONTENT

Supporting Information. Views of the electrochemical cell, cyclic voltammograms of the DNA intercalating redox probes, influence of the DNA intercalating redox probes on the polymerase chain reaction, stability of the SWV peak current response of the DNA intercalating redox probes during thermal PCR cycling, evolution of the SWV peak current response of $[Os(bpy)_2phen]^{2+}$ and MB during PCR amplification of hCMV DNA target, and determination of the affinity binding constant of $[Os(bpy)_2DPPZ]^{2+}$ toward ds-DNA. This material is available free of charge via the Internet at http://pubs.acs.org.

AUTHOR INFORMATION

Corresponding Author

*E-mail: marchal@univ-paris-diderot.fr (D.M.); limoges@ univ-paris-diderot.fr (B.L.).

ACKNOWLEDGMENT

This research was supported by Université Paris Diderot, CNRS, Région Bourgogne (partial Ph.D. financial support of T.D.) and Agence Nationale de la Recherche (ANR-EMPB-DETSCAN project). We thank Argene S.A. for providing their hCMV DNA kit and the TaqMan-based real-time PCR calibration plot.

REFERENCES

(1) (a) Higuchi, R.; Dollinger, G.; Walsh, P. S.; Griffith, R. *Bio/Technology* **1992**, *10*, 413–417. (b) Holland, P. M.; Abramson, R. D.; Watson, R.; Gelfand, D. H. *Proc. Natl. Acad. Sci. U.S.A.* **1992**, *88*, 7276–7280.

(2) Wilhelm, J.; Pingoud, A. *ChemBioChem* **2003**, *4*, 1120–1128.

(3) (a) Higuchi, R.; Fockler, C.; Dollinger, G.; Watson, R. *Biotechnology* **1993**, *11*, 1026–1030. (b) Ririe, K. M.; Rasmussen, R. P.; Wittwer, C. T. *Anal. Biochem.* **1997**, *245*, 154–160.

(4) (a) Tyagi, S.; Kramer, F. R. *Nat. Biotechnol.* **1996**, *14*, 303–308. (b) Livak, K. J.; Flood, S. J.; Marmaro, J.; Giusti, W.; Deetz, K. *Genome Res.* **1995**, *4*, 357–362. (c) Wittwer, C. T.; Herrmann, M. G.; Moss, A. A.; Rasmussen, R. P. *Biotechniques* **1997**, *22*, 130–138. (d) Whitcombe, D.; Theaker, J.; Guy, S. P.; Brown, T.; Little, S. *Nat. Biotechnol.* **1999**, *17*, 804–807. (e) Holland, P. M.; Abramson, R. D.; Watson, R.; Gelfand, D. H. *Proc. Natl. Acad. Sci. U.S.A.* **1991**, *88*, 7276–7280. (f) Sherrill, C. B.; Marshall, D. J.; Moser, M. J.; Larsen, C. A.; Daudé-Snow, L.; Prudent, J. R. *J. Am. Chem. Soc.* **2004**, *126*, 4550–4556.

(5) Hou, C. S. J.; Milovic, N.; Godin, M.; Russo, P. R.; Chakrabarti, R.; Manalis, S. R. *Anal. Chem.* **2006**, *78*, 2526–2531.

(6) (a) Liu, R. H.; Yang, J.; Lenigk, R.; Bonanno, J.; Grodzinski, P. *Anal. Chem.* **2004**, *76*, 1824–1831. (b) Gore, M. R.; Szalai, V. A.; Ropp, P. A.; Yang, I. V.; Silverman, J. S.; Thorp, H. H. *Anal. Chem.* **2003**, *75*, 6586–6592. (c) Ferguson, B. S.; Buchsbaum, S. F.; Swensen, J. S.; Hsieh, K.; Lou, X.; Soh, H. T. *Anal. Chem.* **2009**, *81*, 6503–6508. (d) Yeung, S. S. W.; Lee, T. M. H.; Hsing, I.-M. *J. Am. Chem. Soc.* **2006**, *128*, 13374–13375. (e) Yeung, S. S. W.; Lee, T. M. H.; Hsing, I.-M. *Anal. Chem.* **2008**, *80*, 363–368.

(7) Deféver, T.; Druet, M.; Rochelet-Dequaire, M.; Joannes, M.; Grossiord, C.; Limoges, B.; Marchal, D. *J. Am. Chem. Soc.* **2009**, *131*, 11433–11441.

(8) Unlike SYBR green-based real-time PCR, the method does not allow to check by an end-PCR melting curve analysis that the correct DNA fragments were amplified.

(9) Marchal, D.; Deféver, T.; Limoges, B. Patents FR 2008/03143 and WO 2009/147322, 2008 and 2009.

(10) Kober, E. M.; Caspar, J. V.; Sullivan, B. P.; Meyer, T. *Inorg. Chem.* **1988**, *27*, 4587–4598.

(11) Gouarin, S.; Vabret, A.; Scieux, C.; Agbalika, F.; Cherot, J.; Mengelle, C.; Deback, C.; Petitjean, J.; Dina, J.; Freymuth, F. *J. Virol. Methods* **2007**, *146*, 147–154.

(12) Friedman, A. E.; Chambron, J. C.; Sauvage, J. P.; Turro, N. J.; Barton, J. K. *J. Am. Chem. Soc.* **1990**, *112*, 4960–4962.

(13) Maruyama, K.; Mishima, Y.; Minagawa, K.; Motonaka, J. *Anal. Chem.* **2002**, *74*, 3698–3703.

(14) Fang, T. H.; Ramalingam, N.; Dong, X.-D.; Ngin, T. S.; Zeng, X.; Kuan, A. T. L.; Huat, E. Y. P.; Gong, H.-Q. *Biosens. Bioelectron.* **2009**, *24*, 2131–2136.

(15) (a) Monis, P. T.; Giglio, S.; Saint, C. P. *Anal. Biochem.* **2005**, *340*, 24–34. (b) Gudnason, H.; Dufva, M.; Bang, D. D.; Wolff, A. *Nucleic Acids Res.* **2007**, *35*, No. e127.

(16) (a) Zhang, L. Z.; Tang, G.-Q. *J. Photochem. Photobiol.* **2004**, *74*, 119–125. (b) Baranovskii, S. F.; Bolotin, P. A.; Evstigneev, M. P.; Chernyshev, D. N. *J. Appl. Spectrosc.* **2008**, *75*, 251–259. (c) Nafisi, S; Saboury, A. A.; Keramat, N; Neault, J.-F.; Tajmir-Riahi, H.-A. *J. Mol. Struct.* **2007**, *827*, 35–43. (d) Fujimoto, B. S.; Clendenning, J. B.; Delrow, J. J.; Heath, P. J.; Shurr, M. *J. Phys. Chem.* **1994**, *98*, 6633–6643. (e) Hagmar, P.; Pierrou, S.; Nielsen, P.; Nordén, B.; Kubista, M. *Biomol. Struct. Dynam.* **1992**, *9*, 667–679.

(17) Pierard, F.; Del Guerzo, A.; Mesmaeker, A. K.; Demeunynck, M.; Lhomme, J. *Phys. Chem. Chem. Phys.* **2001**, *3*, 2911–2920.

(18) (a) Yan, X.; Habbersett, R. C.; Cordek, J. M.; Nolan, J. P.; Yoshida, T. M.; Jett, J. H.; Marrone, B. L. *Anal. Biochem.* **2000**, *286*, 138–148. (b) Mao, F.; Leung, W.-Y.; Xin, X. *BMC Biotechnol.* **2007**, *7*, 1–16.

(19) This is supported by the fact that the DNA-bindings of intercalators such as MB or metal bipyridine-based complexes are driven by large favorable enthalpy contributions, with ΔH^0 ranging

from −14 to −76 kJ/mol.[15,18] Yu, H.-J.; Huang, S.-M.; Li, L.-Y.; Jia, H.-N.; Chao, H.; Mao, Z.-W.; Liu, J.-Z.; Ji, L.-N. *J. Inorg. Biochem.* **2009**, *103*, 881–890.

(20) (a) Maruyama, K.; Mishima, Y.; Minagawa, K.; Motonala, J. *Anal. Chem.* **2002**, *74*, 3698–3703. (b) Welch, T. W.; Corbett, A. H.; Thorp, H. H. *J. Phys. Chem.* **1996**, *100*, 13829–13836.

(21) For simplicity, we have considered that the amplification efficiency is constant throughout the whole PCR cycles.

(22) Casabianca, A.; Gori, C.; Orlandi, C.; Forbici, F.; Perno, C. F.; Magnani, M. *Mol. Cell. Probes* **2007**, *21*, 368–378.